Journal of Electrocardiology 99 (2026) 154425

Contents lists available at ScienceDirect

Journal of Electrocardiology

journal homepage: www.jecgonline.com

Performance comparison of parameters characterizing P wave variability before the onset of atrial fibrillation ☆

M. Noriega [a], C. Moreno [a], A. Martín-Yebra [a,b,c], P.G. Platonov [e], A. Savelev [e], J. Marta [d], J.P. Martínez [a,c], L. Sörnmo [f], P. Laguna [a,c,*]

[a] University of Zaragoza, BSICoS group, I3A, IIS-Aragón, Zaragoza, Spain
[b] Fundación ARAID, Zaragoza, Spain
[c] CIBER-BBN, Zaragoza, Spain
[d] Neurovascular Unit, Hospital U. Miguel Servet, IIS Aragon, Zaragoza, Spain
[e] Lund University, Department of Clinical Sciences, Lund, Sweden
[f] Lund University, Department of Biomedical Engineering, Lund, Sweden

ARTICLE INFO

Keywords:
ECG
P wave morphological variability
Atrial fibrillation

ABSTRACT

Short-term characterization of P waves occurring before the onset of atrial fibrillation (AF) is essential to better understand triggering mechanisms. The characterization is challenged by a low signal-to-noise ratio which makes P wave delineation difficult. This study compares the performance of a parameter characterizing P wave morphological variability (MV) to that of four previously published P wave variability parameters: amplitude dispersion, duration, arc length, and power ratio of principal components. The comparison is based on the St. Petersburg Atrial Fibrillation Database comprising 176 one-hour sinus rhythm segments just before AF onset, obtained from 32 patients. Following a linear, spatial transformation that emphasizes the P wave, the MV parameter is computed in consecutive, overlapping subsegments and normalized by a reference value taken one hour before AF onset. The results show that the MV parameter exhibits the highest reactivity to AF onset, with a mean relative increase of 19% 10 min before AF onset, whereas the other four parameters had lower reactivities (amplitude dispersion: 10%, duration: 0%, arc length: 10%, and power ratio: 2%). The conclusion is that the MV parameter better reflects the short-term instability of the atrial substrate than the other parameters.

Introduction

Atrial fibrillation (AF) is the most common sustained arrhythmia in clinical practice, associated with a substantial risk of stroke and cardiovascular mortality [1,2]. In patients with paroxysmal AF, the identification of ECG changes that precede an AF episode is key to understanding the underlying mechanisms and ultimately to facilitate monitoring and prevention strategies.

Short-term P wave dynamics before AF onset have been studied using a variety of parameters. Martínez et al. were the first to analyze the beat-to-beat variability of P wave parameters in a 60-min window before AF onset, showing a progressive increase in variability as AF onset approaches [3,4]. In other studies, the variability of both P wave duration and high-frequency energy (80–200 Hz) were found to increase in the hours before AF onset [5,6]. Filos et al. confirmed these observations using another cohort [7]. Censi et al. evaluated whether temporal P wave variability provides additional information on the atrial substrate associated with AF [8]. Although these studies show that P-wave dynamics can capture pre-AF electrical instability, it remains unclear which variability parameter reflects these short-term changes with the highest reactivity.

From a clinical perspective, ECG-based risk prediction of AF has been extensively investigated in recent decades and then mostly focused on long-term prognostic horizons (several years) using the resting or ambulatory ECG. Various population-based studies have demonstrated that static P wave alterations, e.g., frontal axis, dispersion, or composite amplitude index, are associated with incident AF at medium-term follow-up [9]. Baturova et al. found that an abnormal P wave axis and an elevated, combined morphology, voltage and P wave duration (MVP) index were independent predictors of AF within 5 years [9]. Cortez et al. found that the combination of P wave duration and vector magnitude (Pd/Pvm) predicted AF after stroke [10].

☆ This article is part of a Special issue entitled: 'ISCE' published in Journal of Electrocardiology.

* Corresponding author at: University of Zaragoza, BSICoS group, I3A, IIS-Aragón, Zaragoza, Spain.
E-mail address: laguna@unizar.es (P. Laguna).

https://doi.org/10.1016/j.jelectrocard.2026.154425

Available online 21 August 2026
0022-0736/© 2026 The Authors. Published by Elsevier Inc. This is an open access article under the CC BY-NC license (http://creativecommons.org/licenses/by-nc/4.0/).

The computation of P wave parameters typically requires wave delineation — a task made difficult by the often low signal-to-noise ratio (SNR) of the P wave [11]. Since the large variability reported in these studies can, to some extent, be related to this issue, more robust parameters are needed to capture the variability of physiological origin.

The aim of the present study is to compare the recently proposed P-wave morphological variability (MV) parameter [12] to four published parameters in terms of reactivity to the short-term atrial electrical destabilization that precedes AF; the problem of predicting AF is outside the scope of this study.

Materials and methods

ECG dataset

The study analyzes the St. Petersburg Atrial Fibrillation Database (SPAFDB) [13], consisting of 37 long-term, ambulatory recordings from patients with paroxysmal AF (the mean recording duration is 104 h). The database includes two different three-lead configurations: three unspecified leads and leads I, II, and III. The sampling rate was 500 Hz. The study was approved by a local ethics committee.

Beat type annotation was performed using a commercial CE-approved ECG analysis software (Cardiolund AB, Lund, Sweden). The protocol for AF episode annotation combined machine annotation with manual expert review to detect missed episodes, remove false positives, and improve episode onset and end [13].

ECG preprocessing

The preprocessing involved forward–backward bandpass filtering using a 12:th order Butterworth filter (0.5–40 Hz) to suppress baseline wander, powerline interference, and muscle artifacts. P waves were deemed acceptable for analysis only if the beat SNR exceeded 20 dB, defined as the ratio between the peak-to-peak QRS amplitude and the RMS value of high-frequency noise (>25 Hz) in the surrounding intervals [14]. Then, 60-min segments with sinus rhythm before AF onset were chosen for analysis, while shorter ones were excluded, see below for further details.

P wave enhancement using PCA-based spatial projection

To emphasize the SNR of the P waves, a new lead derived by a linear spatial transformation of the three leads, based on principal component analysis (PCA), was used following the approach described in [12]. The transformation is determined from a representative subset of P waves after which the three leads are projected to produce the transformed leads. The first PCA component, denoted $\mathbf{y}_1 = [y_1(0), \ldots, y_1(M-1)]$ where M is the total number of samples in a 60-min segment, maximizes the P wave energy and presumably its morphological variability, jointly minimizing the noise energy.

P wave segmentation and selection criteria

The variability analysis was performed on normal sinus P waves in each 60-min segment, which in turn was divided into 59 consecutive 2-min subsegments with a 1-min overlap. The parameters were computed in each subsegment provided that the subsegment contained at least 20 acceptable P waves; otherwise, the subsegment was excluded from further analysis. Segments with fewer than 15 acceptable subsegments were excluded. In total, five recordings were excluded: one due to missing AF annotations, one due to the lack of a 60-min sinus rhythm segment, and three due to fewer than 15 acceptable subsegments. Consequently, 32 recordings were analyzed consisting of 176 60-min segments (median [range] of 4 [1,16] segments per recording). In the following, these segments are referred to as *just-before-AF segments*.

A control group was defined by 60-min sinus rhythm segments occurring earlier than the just-before-AF segments, fulfilling the following two criteria: (1) segment onset occurred at least 1 h after the end of the preceding AF episode, and (2) segment end occurred at least 1 h before the onset of the next AF episode. These two criteria resulted in that 171 segments were chosen from 30 of the 32 recordings. In the following, these segments are referred to as *far-from-AF segments*.

The following five index sets are introduced to facilitate the description of parameters:

$$\text{recordings: } i \in \Omega_I = \{1, \ldots, I\}, I = 32, \tag{1}$$

$$\text{segments: } j \in \Omega_J = \{1, \ldots, J_i\}, \tag{2}$$

$$\text{subsegments: } k \in \Omega_K = \{-K, \ldots, -1\}, K = 59, \tag{3}$$

$$\text{PCA-transformed leads: } c \in \Omega_C = \{1, 2, 3\}, \tag{4}$$

$$\text{beat number: } l \in \Omega_L = \{1, \ldots, L_{i,j,k,c=1,l}\}. \tag{5}$$

The negative values in Ω_K indicate time before AF onset.

Segmentation of each P wave $p_{i,j,k,c,l}(n)$ was performed using the criteria found in [12]. A 140-ms window beginning 220 ms before the QRS fiducial point was used, ensuring that the vast part of the P wave is analyzed.

P wave variability parameters

This section describes five P wave variability parameters that are compared with respect to reactivity. For each parameter, the variability is computed as a function of the subsegment index k.

P wave morphological variability

The proposed parameter $V^{\mathrm{MV}}_{i,j}(k)$ characterizing morphological variability (MV) is defined as the energy of the median absolute deviation (MAD) of $p_{i,j,k,c,l}(n)$ of the first transformed lead ($c = 1$), normalized by the median energy of all P waves of the recording:

$$V^{\mathrm{MV}}_{i,j}(k) = \frac{\sum_{n=0}^{N-1} \left(\underset{l \in \Omega_L}{\mathrm{mad}} \left(p_{i,j,k,1,l}(n) \right) \right)^2}{\underset{j \in \Omega_J, k \in \Omega_K, l \in \Omega_L}{\mathrm{median}} \left(\sum_{n=0}^{N-1} p^2_{i,j,k,1,l}(n) \right)}. \tag{6}$$

P wave amplitude dispersion

The amplitude dispersion (AD) is determined from the first transformed lead [8]:

$$V^{\mathrm{AD}}_{i,j}(k) = \frac{\max_n \left(\Delta^{\mathrm{AD}}_{i,j,k,1}(n) \right)}{\max_{n, l \in \Omega_L} \left(p_{i,j,k,1,l}(n) \right)}, \tag{7}$$

where

$$\Delta^{\mathrm{AD}}_{i,j,k,1}(n) = \max_{l \in \Omega_L} \left(p_{i,j,k,1,l}(n) \right) - \min_{l \in \Omega_L} \left(p_{i,j,k,1,l}(n) \right). \tag{8}$$

P wave duration variability

Using the delineator in [15], the P wave duration $d_{i,j,k,1,l}$ is estimated and the variability is determined by the MAD:

$$V^{\mathrm{D}}_{i,j}(k) = \underset{l \in \Omega_L}{\mathrm{mad}} \left(d_{i,j,k,1,l} \right). \tag{9}$$

P wave arc length variability

The arc length $a_{i,j,k,1,l}$ is computed as the P wave path distance from P wave onset to end in the first transformed lead [4] after which the variability is determined by the MAD:

$$V^{\mathrm{A}}_{i,j}(k) = \underset{l \in \Omega_L}{\mathrm{mad}} \left(a_{i,j,k,1,l} \right). \tag{10}$$

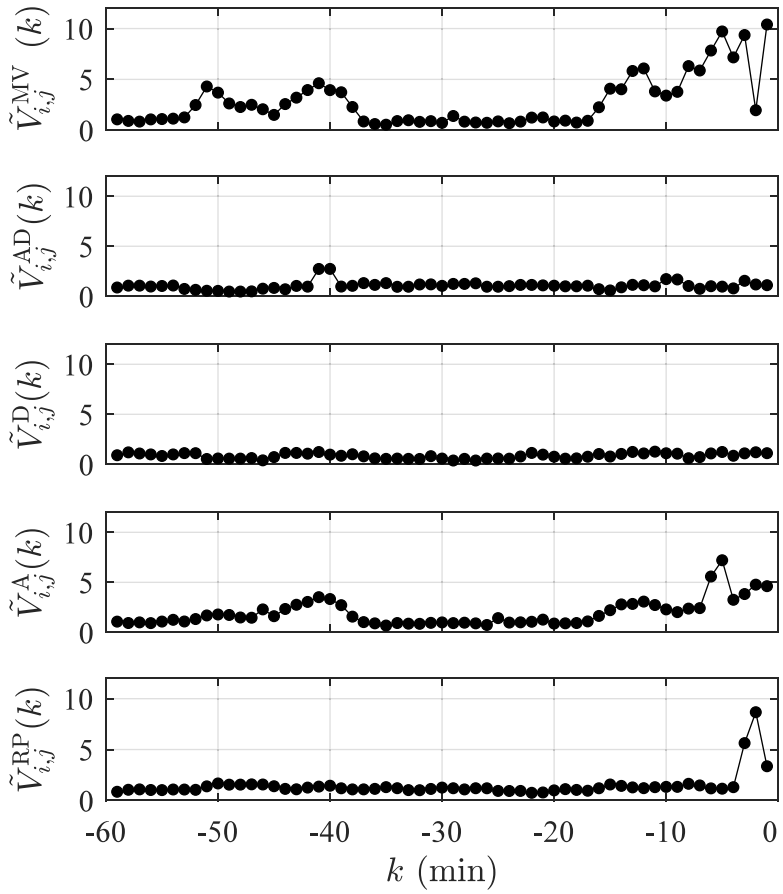


Fig. 1. Illustration of P wave variability in a 60-min just-before-AF segment when characterized by the five parameters.

Relative power of the second-to-first PCA component

The relative power (RP) between an average P wave template determined from the first and second transformed leads was introduced to assess differences in P wave loop circularity [16]. The variability of the RP is defined by:

$$V_{i,j}^{\mathrm{RP}}(k) = \frac{\sum_{n=0}^{N-1} \bar{p}_{i,j,k,2}^{2}(n)}{\sum_{n=0}^{N-1} \bar{p}_{i,j,k,1}^{2}(n)}, \tag{11}$$

where the average P wave template $\bar{p}_{i,j,k,c}(n)$ is given by:

$$\bar{p}_{i,j,k,c}(n) = \frac{1}{L_{i,j,k}} \sum_{l=1}^{L_{i,j,k}} p_{i,j,k,c,l}(n). \tag{12}$$

60-Min before AF normalization

To facilitate an inter-segment comparison, $V_{i,j}^{\mathcal{I}}(k)$ is normalized by a "reference value" for each segment taken as the median of the first 5 min of the segment:

$$\tilde{V}_{i,j}^{\mathcal{I}}(k) = \frac{V_{i,j}^{\mathcal{I}}(k)}{\underset{k=-59,\cdots,-55}{\mathrm{median}}\left(V_{i,j}^{\mathcal{I}}(k)\right)}, \quad \mathcal{I} \in \{\mathrm{MV}, \mathrm{AD}, \mathrm{D}, \mathrm{A}, \mathrm{RP}\}. \tag{13}$$

Reactivity as performance measure

Global analysis has shown that $\tilde{V}_{i,j}^{\mathrm{MV}}(k)$ remains relatively stable until approximately 8 min before AF onset when it typically begins to increase [12]. Based on this finding, the relative increase in variability, referred to as *reactivity*, is computed as the difference between the mean of $\tilde{V}_{i,j}^{\mathcal{I}}(k)$ by the w:th non-overlapping 10 min window before AF onset and the first 5 min of the segment, normalized by the mean of $\tilde{V}_{i,j}^{\mathcal{I}}(k)$ during the first 5 min:

$$\Delta_{i,j}^{\mathcal{I},w} = \frac{\frac{1}{10}\sum_{k=-10w}^{-10(w-1)-1} \tilde{V}_{i,j}^{\mathcal{I}}(k) - \frac{1}{5}\sum_{k=-59}^{-55} \tilde{V}_{i,j}^{\mathcal{I}}(k)}{\frac{1}{5}\sum_{k=-59}^{-55} \tilde{V}_{i,j}^{\mathcal{I}}(k)}. \tag{14}$$

The Wilcoxon signed-rank test was applied exclusively to the just-before-AF segments to determine whether statistically significant differences existed between $\Delta_{i,j}^{\mathrm{MV},w}$ and $\Delta_{i,j}^{\mathcal{I},w}$, $\mathcal{I} \in \{\mathrm{AD}, \mathrm{D}, \mathrm{A}, \mathrm{RP}\}$, $w \in \{1, 2, 3\}$. This test was also used to determine whether $\Delta_{i,j}^{\mathcal{I},w}$ was different from zero with statistical significance.

Complementary discrimination analysis

The discriminative capability of the five parameters was further evaluated by comparing their values computed in just-before-AF segments and far-from-AF sinus rhythm segments. The capability of each parameter was evaluated using the reactivity index $\Delta_{i,j}^{\mathcal{I},1}$, i.e., measured at the window closest to AF onset. Receiver operating characteristics (ROCs) were obtained, along with the corresponding AUC, as well as the sensitivity, specificity, and F1 measured for a given threshold γ.

Firstly, a decision threshold of $\gamma = 0$ was considered, representing the absence of reactivity relative to the reference interval. Secondly, an independent threshold was selected for each variability parameter, defined as the maximum between the median value of $\Delta_{i,j}^{\mathcal{I},1}$, computed in both just-before-AF and far-from-AF segments, and zero. The design of the second threshold is driven by physiology and accounts the entire population.

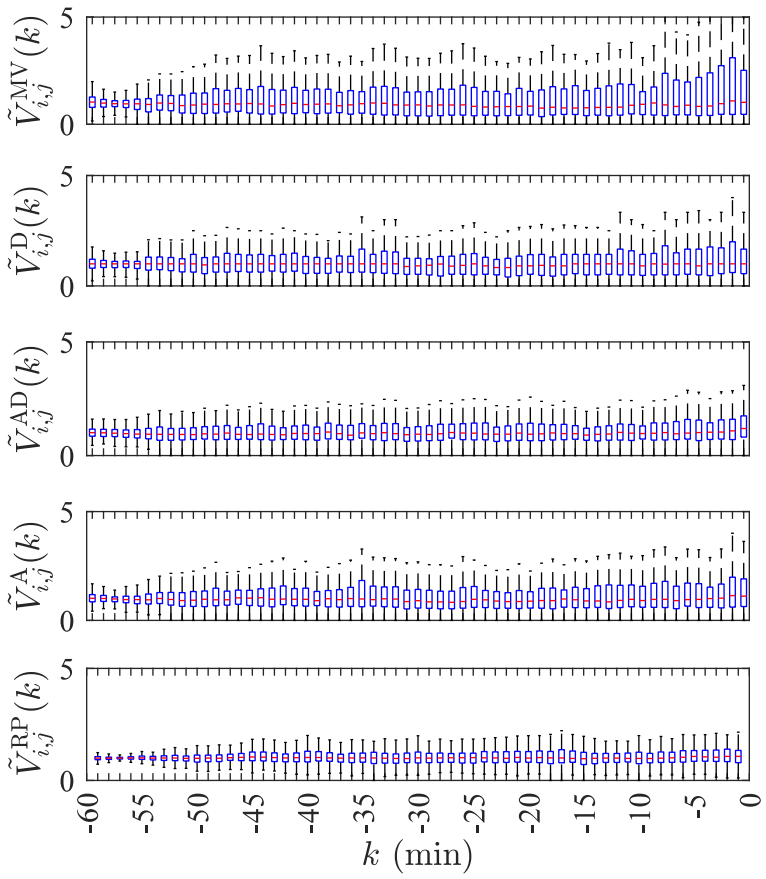


Fig. 2. Boxplot distribution of $\tilde{V}_{i,j}^{\mathcal{I}}(k), \mathcal{I} \in \{\mathrm{MV}, \mathrm{D}, \mathrm{AD}, \mathrm{A}, \mathrm{RP}\}$ based on the 176 segments of SPAFDB.

Results

Temporal analysis of the variability parameters

Fig. 1 illustrates the variability as characterized by each of the five parameters. An increase in variability can be observed for $\tilde{V}_{i,j}^{\mathrm{MV}}(k)$, $\tilde{V}_{i,j}^{\mathrm{A}}(k)$, and $\tilde{V}_{i,j}^{\mathrm{RP}}(k)$ just before AF onset, while $\tilde{V}_{i,j}^{\mathrm{AD}}(k)$ and $\tilde{V}_{i,j}^{\mathrm{D}}(k)$ do not exhibit an increase.

Fig. 2 illustrates the distribution of $\tilde{V}_{i,j}^{\mathcal{I}}(k)$ for all 176 segments. In general, all parameters exhibit a gradual increase as AF onset approaches. The increase is most pronounced for $\tilde{V}_{i,j}^{\mathrm{MV}}(k)$ during the last few minutes, where the largest median [IQR] occurs at $k = -2$; 1.09 [0.46, 3.10]. Although less pronounced, D, AD, and A also exhibit an increase with 1 [0.60, 2.0] at $k = -2$, 1.19 [0.81, 1.75] at $k = -1$, and 1.13 [0.61, 1.98] at $k = -2$ respectively. In contrast, $\tilde{V}_{i,j}^{\mathrm{RP}}(k)$ has a much smaller variation.

Reactivity comparison of variability parameters

Fig. 3 displays the $\Delta_{i,j}^{\mathcal{I},w}$ distributions for the five parameters across the three analyzed time windows (indexed by w) for both just-before-AF and far-from-AF segments. For the former segments, $\Delta_{i,j}^{\mathcal{I},w}$ increased progressively as AF onset is approaching. In contrast, $\Delta_{i,j}^{\mathcal{I},w}$ remained largely unchanged for the latter segments. Notably, $\Delta_{i,j}^{\mathrm{MV},w}$ differed significantly from zero for all three 10-intervals of just-before-AF segments. $\Delta_{i,j}^{\mathrm{MV},1}$ was associated with the largest relative change, with a median [IQR] of 0.19 $[-0.43, 1.64]$.

$\Delta_{i,j}^{\mathrm{AD},w}$ also differed significantly from zero in all three intervals, albeit with a lower magnitude than $\Delta_{i,j}^{\mathrm{MV},w}$ (0.1, $[-0.20, 0.46]$ for $w = 1$). In contrast, $\Delta_{i,j}^{\mathrm{D},w}$ and $\Delta_{i,j}^{\mathrm{A},w}$ only reached statistical significance for $w = 1$ (0 $[-0.38, 0.72]$ and 0.1 $[-0.34, 0.77]$, respectively), whereas RP showed no significant differences from zero in any segment.

Pairwise comparisons showed that $\Delta_{i,j}^{\mathrm{MV},w}$ in just-before AF segments yielded significantly higher values than the remaining parameters for $w = 1$. For $w = 2$ and 3, the statistical superiority of $\Delta_{i,j}^{\mathrm{MV},w}$ persisted against $\Delta_{i,j}^{\mathrm{D},w}$ in both intervals and against $\Delta_{i,j}^{\mathrm{A},w}$ for $w = 3$ only.

Table 1
Sensitivity, specificity, and F1 scores obtained for the evaluated methods for the decision threshold $\gamma = 0$.

Method	Sen. (%)	Sp. (%)	F1 (%)
MV	**56.8**	56.7	57.1
D	48.3	67.8	53.8
AD	55.1	62.6	57.5
A	52.2	57.3	53.9
RP	50.6	60.8	53.6

Discrimination analysis

Fig. 4 shows the ROCs for discriminating between just-before-AF and far-from-AF segments. All parameters exhibited moderate discriminative capacity (AUC range: 0.57–0.63). AD yielded the highest AUC (0.626), followed by MV (0.579), RP (0.574), and both A and D (0.573).

Table 1 summarizes the sensitivity and specificity at the canonic decision threshold ($\Delta_{i,j}^{\mathcal{I},1} = 0$). MV yielded the highest sensitivity (56.8%), followed by AD (55.1%), A (52.3%), RP (50.6%), and D (48.3%). For specificity, D and AD achieved the highest values (67.8% and 62.6%, respectively). AD and MV achieved the highest F1 scores, at 57.5 and 57.1, respectively.

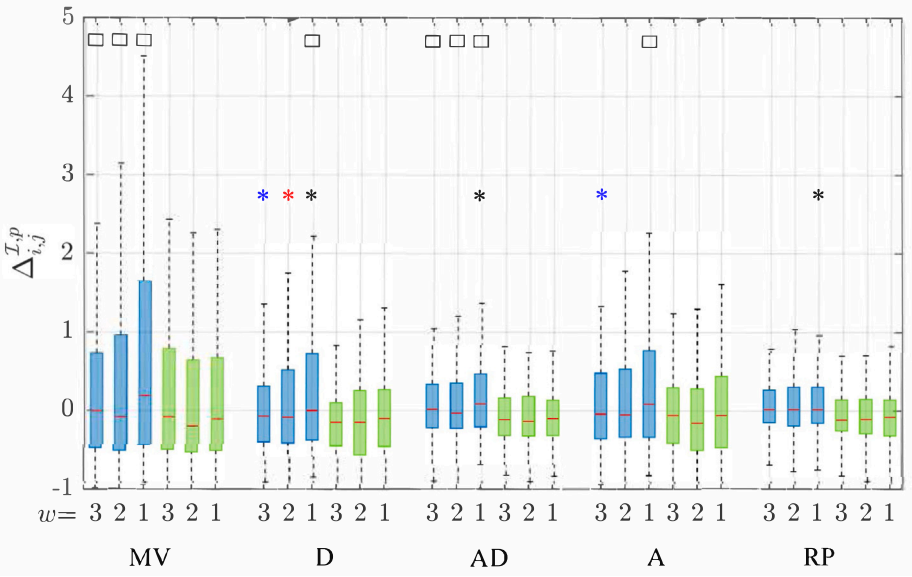


Fig. 3. Boxplot distributions of $\Delta_{i,j}^{\mathcal{I},w}$ for different parameters. The results from analyzing just-before-AF and far-from-AF segments are displayed in blue and green, respectively. The asterisk indicates a difference relative to the corresponding $\Delta_{i,j}^{\mathrm{MV},w}$ with statistically significance. The rectangle indicates that $\Delta_{i,j}^{\mathcal{I},w}$ differs from 0 with statistically significance. (For interpretation of the references to color in this figure legend, the reader is referred to the web version of this article.)

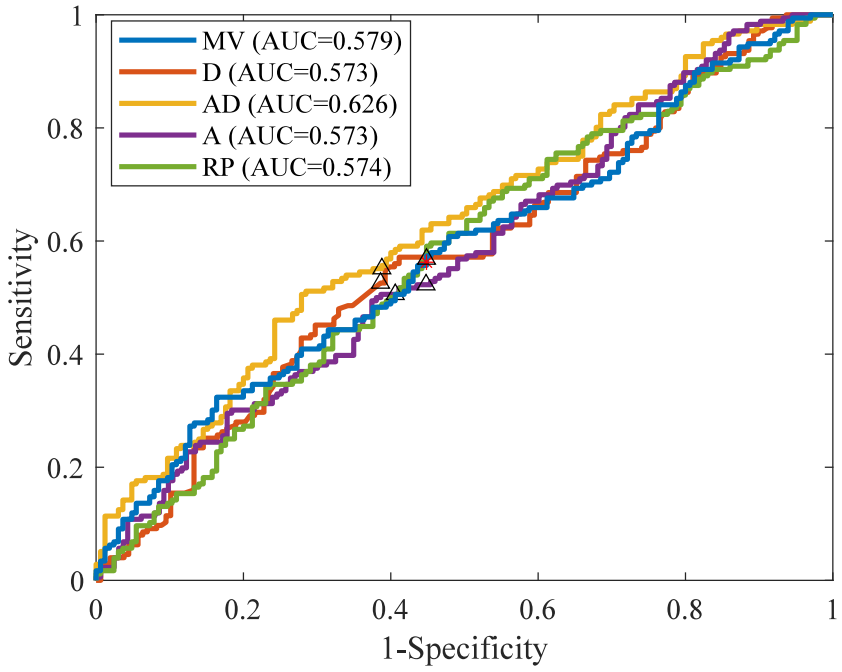


Fig. 4. ROCs obtained for the five P wave variability parameters. The reactivity index $\Delta_{i,j}^{\mathcal{I},1}$ was used as discriminatory variable. The black triangle denotes the threshold $\gamma = 0$. The red asterisk denotes the $\gamma = 0.03$ threshold for MV. (For interpretation of the references to color in this figure legend, the reader is referred to the web version of this article.)

In the second classification approach, the median of $\Delta_{i,j}^{\mathcal{I},1}$ for all segments was 0.03, −0.1, −0.02, −0.02, and −0.03 for MV, D, AD, A, and RP, respectively. Consequently, the independent thresholds selected in this case remained zero for D, AD, A, and RP, and 0.03 for MV. Using these thresholds, MV resulted in a sensitivity of 56.5%, a specificity of 57.3%, and F1 of 56.5%, thus remaining the parameter offering the highest sensitivity. AD maintained its role as the best parameter for identifying far-from-AF segments.

Discussion

Identification of short-term temporal characteristics before AF onset remains an important challenge, particularly given the uncertainty associated with low signal-to-noise ratios. Addressing this need, the present study investigates the reactivity of five parameters characterizing the atrial electrical instability before AF onset.

Temporal distribution and relative increase of $\tilde{V}_{i,j}^{\mathcal{I}}(k)$

As illustrated by Fig. 2, all parameters exhibit an increase as AF onset approaches, however, $\tilde{V}_{i,j}^{\mathrm{MV}}(k)$ demonstrates the most pronounced increase in both median and dispersion. The additional temporal analysis of the reactivity index $\Delta_{i,j}^{\mathcal{I},w}$ further shows in just-before-AF segments that this increase is progressive as AF onset approaches rather than restricted to the last 10 min before the episode ($w = 1$). MV exhibits statistically significant reactivity with respect to the reference interval in all three time windows, whereas D and A become significant only during the last 10 min before AF onset. AD also remains significantly different from zero throughout the analyzed period, although with lower reactivity than MV. Moreover, MV maintains significantly higher reactivity than the remaining parameters in most pairwise comparisons, with the largest differences observed during the last 10 min before AF onset, where the median of $\Delta_{i,j}^{\mathrm{MV},1}$ reaches 0.19, being the largest increase in reactivity.

This finding suggests that the electrical destabilization before AF onset is manifested more robustly through alterations in the overall P wave morphology, captured as the MAD energy, than through parameters dependent on duration, amplitude, or arc length. The progressive increase in MV reactivity in the three windows further suggests that the destabilization develops gradually before AF onset rather than immediately before AF onset. Although $\tilde{V}_{i,j}^{\mathrm{D}}(k)$ and $\tilde{V}_{i,j}^{\mathrm{A}}(k)$ exhibit statistically significant increases with respect to zero during the last 10 min before AF onset, their lower reactivity may be attributed to their susceptibility to delineation errors; a limitation recognized in the literature [11]. Considering the temporal structure of the P wave, $\tilde{V}_{i,j}^{\mathrm{MV}}(k)$ mitigates the impact of transient noise and therefore should provide better characterization of the atrial substrate. It should be noted that $\Delta_{i,j}^{\mathrm{D},1}$ has a median of zero, indicating an increase in P wave duration in this time interval not observed in at least 50% of all segments immediately before AF onset.

Although AD shows statistically significant reactivity relative to the baseline over all three time windows, its lower magnitude compared to MV may indicate that beat-to-beat variation in P-wave amplitude captures only part of the electrical instability before AF onset.

The low reactivity observed for $\tilde{V}_{i,j}^{\mathrm{RP}}(k)$, manifested by the lack of statistical significance, suggests that AF onset is not characterized primarily by a shift in the spatial distribution of the energy. Since the second PCA component captures the most relevant variations not accounted for by the dominant P wave morphology (captured by the first PCA component) [17], the relatively low reactivity of the power ratio between the second and first components indicates that the changes before AF onset are not adequately reflected in the relative contribution of the second component, but are likely linked to variations in the dominant morphology.

The complementary analysis show that the AD parameter performs slightly better than the MV parameter when evaluated as a standalone classifier. However, the MV parameter yields higher sensitivity across both classification strategies. These results corroborate the manuscript's main findings regarding MV's better reactivity.

Notably, the increasing dispersion in Figs. 2 and 3 as AF onset approaches indicates that not all just-before-AF segments follow a similar temporal trajectory. While many episodes exhibit increased parameter variability immediately before AF, others remain near baseline. This points to heterogeneous variability patterns, consistent with the known existence of distinct triggering mechanisms.

This heterogeneity may partly explain the moderate sensitivity observed for all five parameters. Future studies should investigate these temporal patterns, e.g., via clustering approach, in larger, independent cohorts to better understand AF onset. While our results support MV as a more reactive marker of short-term atrial electrical destabilization, they do not demonstrate the clinical utility of MV as a standalone AF predictor. Rather, MV could constitute a promising component in future multiparametric prediction for use in ambulatory ECG monitoring.

In addition to the small cohort size, the varying number of just-before-AF segments per patient is a limitation of the study, and no correction for within-patient correlation was applied. However, because all parameters were evaluated using the same set of segments, the validity of their relative comparison is preserved. Future studies with larger cohorts should account for patient-level clustering using appropriate statistical approaches.

Conclusion

The MV parameter was found to be the most reactive to atrial electrical destabilization, with a mean relative increase of 19% in the 10 min before AF onset relative to the reference time. Furthermore, its reactivity was considerably higher than those of the other four parameters, with a difference of at least 9%. In terms of statistical significance, the results demonstrate that the MV parameter captures short-term atrial electrical destabilization with greater reactivity than P wave duration, arc length, amplitude dispersion, and PCA power ratio. However, the difference in performance was found to be rather modest when evaluating the parameters as standalone classifiers.

CRediT authorship contribution statement

M. Noriega: Writing – review & editing, Writing – original draft, Visualization, Validation, Software, Methodology, Investigation, Formal analysis, Conceptualization. **C. Moreno:** Software, Methodology. **A. Martín-Yebra:** Writing – review & editing, Investigation, Formal analysis. **P.G. Platonov:** Writing – review & editing, Investigation. **A. Savelev:** Data curation. **J. Marta:** Writing – review & editing. **J.P. Martínez:** Writing – review & editing, Supervision, Methodology, Investigation. **L. Sörnmo:** Writing – review & editing, Supervision, Methodology, Conceptualization. **P. Laguna:** Writing – review & editing, Supervision, Resources, Project administration, Methodology, Funding acquisition, Formal analysis, Conceptualization.

Acknowledgment

This work was supported by the European Union's Horizon Europe programme under the Marie Skłodowska-Curie GA No:101150167 - MESMODI-BCG- and under project PID2022-140556OB-I00 from MICIN, and CIBER-BBN and BSICoS Reference Group (T39-23R) and ARAID Foundation, from Aragon Government, Spain. The computation was performed at the High Performance Computing Platform of the NANBIOSIS ICTS.

References

[1] Wolf PA, Abbott RD, Kannel WB. Atrial fibrillation as an independent risk factor for stroke: The Framingham study. Stroke 1991;22(8):983–8. http://dx.doi.org/10.1161/01.STR.22.8.983.

[2] Harrison SL, Fazio-Eynullayeva E, Lane DA, Underhill P, Lip GYH. Atrial fibrillation and the risk of 30-day incident thromboembolic events, and mortality in adults ≥ 50 years with COVID-19. J Arrhythm 2021;37(1):231–7. http://dx.doi.org/10.1002/joa3.12458.

[3] Martínez A, Alcaraz R, Rieta JJ. Study on the P-wave feature time course as early predictors of paroxysmal atrial fibrillation. Physiol Meas 2012;33(12):1959. http://dx.doi.org/10.1088/0967-3334/33/12/1959.

[4] Martínez A, Alcaraz R, Rieta JJ. Morphological variability of the P-wave for premature envision of paroxysmal atrial fibrillation events. Physiol Meas 2014;35:1–14. http://dx.doi.org/10.1088/0967-3334/35/1/1.

[5] Alcaraz R, Martínez A, Rieta JJ. The p wave time-frequency variability reflects atrial conduction defects before paroxysmal atrial fibrillation. Ann Noninvasive Electrocardiol 2015;20(5):433–45. http://dx.doi.org/10.1111/anec.12240.

[6] Alcaraz R, Martínez A, Rieta JJ. Role of the P-wave high frequency energy and duration as noninvasive cardiovascular predictors of paroxysmal atrial fibrillation. Comput Methods Programs Biomed 2015;119(2):110–9. http://dx.doi.org/10.1016/j.cmpb.2015.01.006.

[7] Filos D, Chouvarda I, Tachmatzidis D, Vassilikos V, Maglaveras N. Beat-to-beat P-wave morphology as a predictor of paroxysmal atrial fibrillation. Comput Methods Programs Biomed 2017;151:111–21. http://dx.doi.org/10.1016/j.cmpb.2017.08.016.

[8] Censi F, Corazza I, Reggiani E, Calcagnini G, Mattei E, Triventi1 M, Boriani G. P-wave variability and atrial fibrillation. Sci Rep 2016;6:26799. http://dx.doi.org/10.1038/srep26799.

[9] Baturova MA, Cornefjord G, Carlson J, Johnson LS, Smith JG, Platonov PG. P-wave characteristics as electrocardiographic markers of atrial abnormality in prediction of incident atrial fibrillation—The Malmö Preventive Project. J Electrocardiol 2024;82:125–30. http://dx.doi.org/10.1016/j.jelectrocard.2023.12.003.

[10] Cortez D, Baturova M, Lindgren A, Carlson J, Shubik YV, Olsson B, Platonov PG. Atrial time and voltage dispersion are both needed to predict new-onset atrial fibrillation in ischemic stroke patients. BMC Cardiovasc Disord 2017;17(1):200. http://dx.doi.org/10.1186/s12872-017-0631-1.

[11] Sörnmo L, editor. Atrial Fibrillation from an Engineering Perspective. Series in Bioengineering, Springer. 2018, http://dx.doi.org/10.1007/978-3-319-68515-1.

[12] Noriega M, Martín-Yebra A, Savelev A, Platonov P, Marta J, Butkuviene M, Martínez JP, Laguna P. P-wave morphological variability exacerbation prior to atrial fibrillation episodes. In: 2025 computing in cardiology. cinC, Vol. 52, 2025, p. 1–4. http://dx.doi.org/10.22489/CinC.2025.084.

[13] Henriksson M, Martín-Yebra A, Butkuvienė M, Rasmussen JG, Marozas V, Petrėnas A, Savelev A, Platonov PG, Sörnmo L. Modeling and estimation of temporal episode patterns in paroxysmal atrial fibrillation. IEEE Trans Biomed Eng 2021;68:319–29. http://dx.doi.org/10.1109/TBME.2020.2995563.

[14] Mincholé A, Sörnmo L, Laguna P. Detection of body position changes from the ECG using a Laplacian noise model. Biomed Signal Proc Control 2014;14:189–96. http://dx.doi.org/10.1016/j.bspc.2014.08.002.

[15] Martínez J, Almeida R, Olmos S, Rocha A, Laguna P. A wavelet-based ECG delineator: Evaluation on standard databases. IEEE Trans Biomed Eng 2004;51(4):570–81. http://dx.doi.org/10.1109/TBME.2003.821031.

[16] Moreno C, Martín-Yebra A, Savelev A, Platonov P, Laguna P, Martínez JP. Analysis of P-wave changes for prediction of atrial fibrillation episodes. In: 2022 computing in cardiology. cinC, Vol. 498, 2022, p. 1–4. http://dx.doi.org/10.22489/CinC.2022.320.

[17] Castells F, Laguna P, Sörnmo L, Bollmann A, Roig JM. Principal component analysis in ECG signal processing. J Adv Signal Process 2007;2007:074580. http://dx.doi.org/10.1155/2007/74580.